Supplemental Material: Movies

Movie 1. Rounding up of an ectodermal aggregate. Cells are labeled with a membrane marker (Gap43-GFP). The movie shows rounding-up of an aggregate over time in a single z-slice. (10 fr/sec.)

Movie 2. Fusion of two ectodermal aggregates. This brightfield movie shows tissue fusion in the equatorial plane of the aggregates. (10 fr/sec.)

Movie 3. Short-term compression of a MZoep ectoderm aggregate. The aggregate behaves elastically and immediately rounds up upon release (real time).

Movie 4. Long-term compression of a MZoep ectoderm aggregate. The aggregate remains flattened upon release. The movie was paused for 1h10min between onset of compression and release of the plates.

Movie 5. Cell sorting of ectodermal cells (red) and mesendodermal cells (green) in a hanging drop experiment. Cell sorting starts almost immediately upon intermixing. As sorting proceeds, the aggregate rounds up to minimize the overall free surface area. Total duration: 8h.


Movie 6. Engulfment of ectoderm tissue (red) by mesendodermal cells (green) in a hanging drop experiment. Engulfment starts almost immediately after aggregate fusion. While engulfment proceeds, the overall shape of the aggregate pair becomes spherical. Total duration: 5h.

Supplemental Figures

Figure S1. Left. Expression of the posterior axial mesoderm (notochord) marker *notail* (*ntl*) assessed by *in situ* hybridization. *Notail* is expressed all around the blastoderm margin at the shield stage in wild type embryos (a), but is lacking dorsally in MZoep (b) and Lefty (c) embryos. **Right.** Expression of the prechordal mesoderm marker *goosecoid* (*gsc*), the mesendoderm marker *mezzo*, the endoderm marker *sox17*, and the ectoderm marker *gata2*. The cyc-aggregates show a strong expression of all the markers, except gata2. In contrast, MZoep aggregates express *gata2* only, while the other markers are absent. The two upper rows are cyc-aggregates immediately after rounding up and 6-7h later. The lower two rows correspond to MZoep aggregates, again immediately after rounding up and 6-7h later. We did not find a significant change in expression pattern over time; *mezzo* expression seemed to be slightly

Figure S2. Cell sorting and envelopment controls. A and B: Cluster formation and cell sorting on fibronectin substrate plated zebrafish ectoderm and mesendoderm cells. (A) Control. MZoep cells, half labeled in red and half in green, form an intermixed aggregate on the fibronectin-coated substrate (12h). (B) Mixed mesendoderm cells (green) and ectoderm cells (red) aggregate and sort out with the ectodermal cells occupying the interior position (12h).

C and D: Sorting of zebrafish mesendoderm and ectoderm from an alternate genetic background. (C) Non-sorting of lefty ectoderm (red) and MZoep ectoderm (green) at 16h. (D) Sphere-within-a-sphere configuration of sorted lefty mRNA-induced ectoderm (red) and cyclops mRNA-induced mesendoderm (green) at 16h. Scale bar = 150 μm.
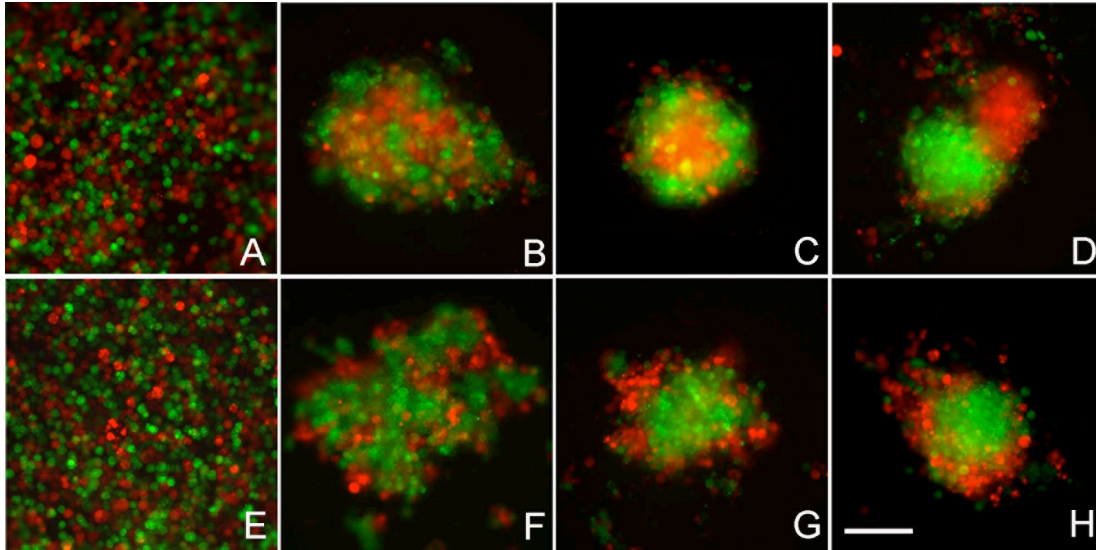
Figure S3. Time course of cell sorting of a small aggregate (10^3-10^4 cells). A-D show the time course of cell sorting for mixed MZoep ectoderm (red) and cyclops-mRNA induced mesendoderm (green) over 24h. E-H show the same time course for a mixture of MZoep+E-cadherin morpholino (red) and mesendoderm (green) cells. In both cases, cells required 1-2 hours in order to coalesce and to cluster at the bottom of the hanging drop (A and E). After 4h in culture (B, F), the tissue with the higher surface tension had already formed large interconnected islands in the interior of the forming aggregate. After approximately 8 hours of incubation, (C, G) cells within the aggregate had rearranged into a sphere-with-a-sphere configuration with ectoderm (C) or mesendoderm (G) adopting the interior position. Panel D represents tissue separation after 20 hours of incubation of mixed ectoderm and mesendoderm. This phase separation did not take place for the E-cadherin morpholino case (H). Images were captured with an epifluorescence microscope. Scale bar = 150 μm for all images.
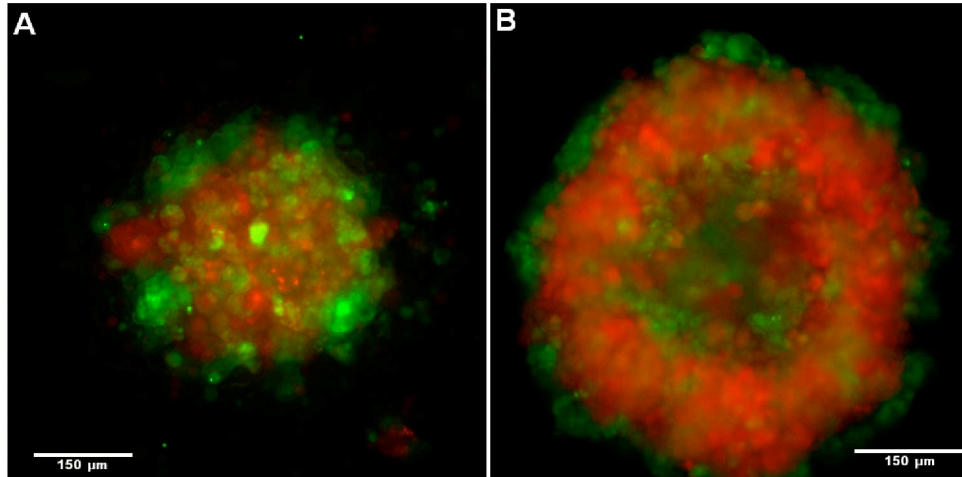
Figure S4. Comparison of cell sorting for two different sized aggregates of MZoep ectoderm (red) and cyclops mRNA-induced mesendoderm (green) cells after 6h in hanging drop culture. While the smaller aggregate (A) is nearly sorted completely, the larger aggregate (B) still has a population of mesendoderm cells in its interior. However, the tendency for mesendoderm to envelop ectoderm is clearly apparent. The ratio of radii of large to small aggregate is, r=1.6. Both images were captured on an inverted epifluorescence microscope.

Figure S5. Partial envelopment (A-C) of mesendoderm by E-cadMO ectoderm and complete envelopment (D-F) of mesendoderm by E-cadMO ectoderm at medium versus high E-cadherin morpholino concentrations. B-C and E-F show the individual channels, for mesendoderm (green) and ectoderm-E-cadMO (red), respectively. Scale bar = 150 μm.
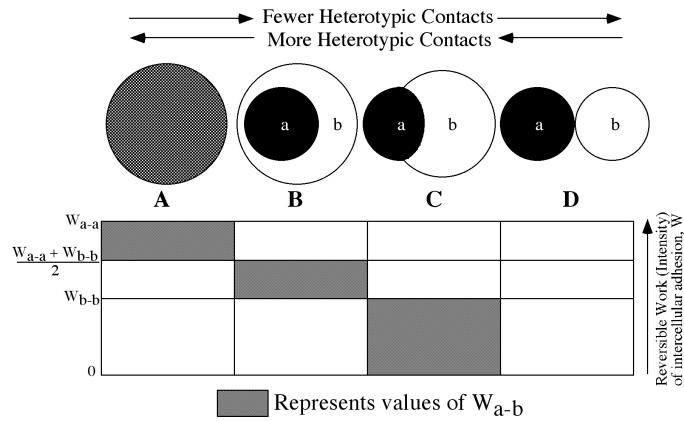
Figure S6. The figure depicts, for a two-phase liquid system, the equilibrium configurations determined by different sets of Ws. By convention, when the two phases differ in cohesiveness, the more cohesive phase is designated *a,* and the less cohesive phase is designated *b.* In the figure, W_{a-a} and W_{b-b} are represented as having higher and lower arbitrary values represented by horizontal solid lines. The figure is divided into four vertical areas, the shading representing a range of values of W_{a-b} from infinity (column A) to zero (column D). A high value of W_{a-b} (higher than the mean of W_{a-a} and W_{b-b}) causes the two phases to mix preferentially (column A). Zero adhesion between *a* and *b* subunits (column D) causes phases *a* and *b* to round up into separate, isolated spheres. Low but positive values of W_{a-b} (between 0 and W_{b-b}) lead to a partial envelopment of phase *a* by phase *b* (column C), while higher values of W_{a-b} (above W_{b-b} but below the average of W_{a-a} and W_{b-b}) lead to complete envelopment of phase *a* by phase *b* (column B), after (Steinberg, 1978).

Supplemental Material – Additional Discussion

1. Cell sorting on longer time-scales.

The current study explored whether differential adhesion could explain the spatial positioning of zebrafish germ layer tissues within a specific time-frame of 4-16h. In this time frame, sorting of mesendoderm and ectoderm resulted in a stable configuration of complete envelopment of ectoderm by the mesendoderm. However, after 20-48h, depending on the number of cells, these tissues separated from each other, resulting in near-complete separation (Supplemental figure Fig. S3D). Interestingly, tissue separation did not occur when mesendoderm cells were mixed with ectoderm+Ecad-MO cells (Supplemental Material, Fig.S3H). Here, the sphere-within-a-sphere configuration persisted beyond 24h. Rearrangement of the tissues from the complete envelopment to the separated state can be explained by a decrease in cross-affinity between the tissue pair, as described in Fig.S6. The fact that the combination of mesendoderm and ectoderm+Ecad-MO did not separate suggests that the rearrangement of the tissues from the complete envelopment to the separated state is due to a change in cohesivity of the mesendodermal but not the ectodermal tissue. This observation may be important for the study of later developmental tissue positioning events, such as the separation of endoderm from mesoderm.

2. Considerations on the order of magnitude of surface and interfacial tensions and cell sorting/tissue engulfment.

In order to predict the final configuration of a heterogeneous cell mixture, two parameters, the surface and interfacial tension, must be known. Together these parameters determine the extent to which cell populations intermix. In 1978, Steinberg provided the conceptual framework of how the interplay between surface and interfacial tension determines the most stable configuration of any multi-subunit system that adopts liquid-like equilibrium shapes, whether the subunits are molecules or cells (Steinberg, 1978). Fig. S6 represents a theoretical framework in which Wa-b, the work of adhesion, is a measure of the cross-adhesion intensity between subunits a and b. This model considers only the simplest scenario assuming isodiametric adhesion molecule expression by all cells. The adhesive relationships between the cells are expressed here not as σ's but as the reversible work of cohesion and adhesion (W), which can be derived from the surface and interfacial tensions (Davies and Rideal, 1963) according to the

$$W_a = 2\sigma_{a0}$$
$$W_b = 2\sigma_{b0}$$
$$W_{ab} = \sigma_{a0} + \sigma_{b0} - \sigma_{ab}$$

Here, σ_{a0} and σ_{b0} denote the measurable surface tensions between the tissue a or b, respectively, and the cell culture medium. σ_{ab} denotes the interfacial tension between the phases a an b.

In the experiments presented in this manuscript, the intermixed state represents a high value of W_{a-b} (higher than the mean of W_{a-a} and W_{b-b}). What we term the "enveloped state" corresponds to a value of Wa-b, which is lower than for the intermixed state. Lower values of Wa-b resulting in partial envelopment, while higher values of W_{a-b} (above W_{b-b} but below the average of W_{a-a} and W_{b-b}) leads to complete envelopment of phase *a* by phase *b* (column B). What we term the "separated state" represents very low or effectively no cross-adhesion between cells. (Steinberg, 1978).

We know from previous studies that zebrafish mesendoderm and ectoderm tissues express E-cadherin and hence have the capacity to interact, effectively generating some value of Wa-b (Babb et al., 2001; Babb and Marrs, 2004; Ulrich et al., 2005). We also know from our previous studies that tissues of lower surface tension always envelop those of higher surface tension (Foty et al., 1996; Foty and Steinberg, 2005). For our zebrafish tissues, we could therefore predict that mesendoderm would envelop ectoderm and would in turn be enveloped by Ecad-MO ectoderm. As shown in the Material and Methods section of this manuscript, surface and interfacial tensions also determine the contact angle between the tissues (Young equation). Mesendoderm envelops ectoderm tissue completely, resulting in a zero contact angle, and thus leads to an estimate of the interfacial tension of $\sigma_{IT} \leq 0.32$ dyne/cm. In the other case, where the phases are reversed, i.e. mesendoderm is internal and surrounded by ectoderm+E-cadherin morpholino (E-cadMO), the situation depends largely on the amount of E-cadMO injected.

We used two populations of E-cadMO treated ectoderm tissues. For medium injection doses (4-6ng) of E-cadherin morpholino in the ectoderm, we observed a drastically reduced surface tension compared to the original tissue, even below the value for the mesendoderm. In

(Ectoderm/Ecad-MO Ectoderm) or partial envelopment of mesendoderm by E-cadMO ectoderm. (Fig. S5 A-C). For higher injection doses (8-9ng) of E-cadherin morpholino (E-cadMO) in the ectoderm, tissues did not round up, and thus TST measurements of their surface tension were impossible. In the cell sorting assays, these cells sorted from both ectoderm and mesendoderm, and attained a complete envelopment configuration (see Fig. 4 and Fig. S5 D-F). Since we have only measured the surface tension for the medium E-cadherinMO doses in the ectoderm, we can only estimate a value range for the interfacial tension between mesendoderm (M) and ectoderm+E-cadherin morpholino (EMO), based on the partial envelopment:

$$\sigma_M - \sigma_{EMO} < \sigma_{M-EMO} < \sigma_M + \sigma_{EMO}.$$

Here, σ_M and σ_{EMO} denote the measured surface tension values against cell culture medium, and σ_{M-EMO} the interfacial tension between the tissues. With the experimentally determined surface tension values we obtain as an estimate for the interfacial tension between mesendoderm and ectoderm+E-cadherin morpholino: 0.11 dyne/cm < σ_{M-EMO} < 0.75 dyne/cm.

A quantitative comparison of the final sorting/engulfment configurations achieved at the two E-cadherinMO doses used in this study shows that partial envelopment and sorting can be distinguished quantitatively from the intermixed state and complete envelopment. N=10 images of each type were analyzed as described in the Materials and Methods section, and the following results were obtained for the envelopment of mesendoderm (green) by ectoderm+ E-cadherinMO (red):

a) partial envelopment: P=(0.41 ± 0.09) and S=(1.39 ± 0.07)

b) complete envelopment: P=(0.12 ± 0.04) and S=(1.51 ± 0.06)

The ratio of scattering amplitudes, S, is larger than one in both cases, by definition: S = S_{red}/S_{green}. While the S-values are equal within errorbars, the P-values are significantly different.